

Linköping University Post Print

Bias mediated tuning of the detection wavelength in asymmetrical quantum dots-in-a-well infrared photodetectors

Linda Höglund, Per-Olof Holtz, H. Pettersson, C. Asplund, Q. Wang, H. Malm, S. Almqvist, E. Petrini and J. Y. Andersson

N.B.: When citing this work, cite the original article.

Original Publication:

Linda Höglund, Per-Olof Holtz, H. Pettersson, C. Asplund, Q. Wang, H. Malm, S. Almqvist, E. Petrini and J. Y. Andersson, Bias mediated tuning of the detection wavelength in asymmetrical quantum dots-in-a-well infrared photodetectors, 2008, Applied Physics Letters, (93), 203512.

<http://dx.doi.org/10.1063/1.3033169>

Copyright: American Institute of Physics

<http://www.aip.org/>

Postprint available at: Linköping University Electronic Press

<http://urn.kb.se/resolve?urn=urn:nbn:se:liu:diva-15769>

Bias mediated tuning of the detection wavelength in asymmetrical quantum dots-in-a-well infrared photodetectors

L. Höglund,^{1,a)} P. O. Holtz,² H. Pettersson,^{3,4} C. Asplund,⁵ Q. Wang,¹ H. Malm,⁵ S. Almqvist,¹ E. Petrini,¹ and J. Y. Andersson¹

¹*Acreo AB, Electrum 236, S-16440 Kista, Sweden*

²*Department of Physics, Chemistry, and Biology (IFM), Linköping University, S-58183 Linköping, Sweden*

³*Center for Applied Mathematics and Physics, Halmstad University, P.O. Box 823,*

S-30118 Halmstad, Sweden

⁴*Sweden Solid State Physics and the Nanometer Consortium, Lund University, P.O. Box 118,*

S-22100 Lund, Sweden

⁵*IRnova, Electrum 236, S-16440 Kista, Sweden*

(Received 1 October 2008; accepted 28 October 2008; published online 21 November 2008)

Bias-mediated tuning of the detection wavelength within the infrared wavelength region is demonstrated for quantum dots-in-a-well and dots-on-a-well infrared photodetectors. By positioning the InAs quantum dot layer asymmetrically in an 8 nm wide In_{0.15}Ga_{0.85}As/GaAs quantum well, a shift in the peak detection wavelength from 8.4 to 10.3 μm was observed when reversing the polarity of the applied bias. For a dots-on-a-well structure, the peak detection wavelength was tuned from 5.4 to 8 μm with small changes in the applied bias. These tuning properties could be essential for applications such as modulators and dual-color infrared detection. © 2008 American Institute of Physics. [DOI: 10.1063/1.3033169]

Cameras for detection of infrared radiation are a growing market with applications in areas such as night vision, surveillance, search and rescue, and medical diagnosis. For infrared detectors, there are two important wavelength regions that have high transmission in the atmosphere; the medium wavelength infrared (MWIR) (3–5 μm) region and the long wavelength infrared (LWIR) (8–14 μm) region. The interest has been focused mainly on single band detectors operating in one of these two wavelength regions. However, additional advantages can be achieved from simultaneous detection in the two different wavelength bands. For example, objects can be identified by their optical signature and remote sensing of the absolute temperature of the scene is enabled.¹

Several approaches among the quantum well (QW) infrared photodetectors have been investigated, including stacking of several QW detector structures designed for different wavelength regions. The different regions can then either be contacted separately for parallel readout^{2,3} or if sequential readout is preferred, different detector structures can be separately addressed by changing the applied bias.^{4–6} In recent years, a new class of infrared detectors has been introduced, so-called quantum dots-in-a-well (DWELL) detectors.⁷ These detectors allow a more advanced approach for sequential dual color detection, involving two different intersubband transitions, which dominate the response at different applied biases; a bound-to-bound transition between a quantum dot (QD) state and a QW subband and bound-to-continuum transitions with final states in the surrounding matrix (corresponding to the LWIR and the MWIR response, respectively).⁸

In this article, two different approaches to improve the tunability of DWELL structures will be presented. In the first approach, an asymmetrically positioned InAs QD layer in a QW enables a bias tunable energy separation between the

QD energy level and QW energy band, resulting in tunability of the detection wavelength within the LWIR wavelength band. In a second approach, the QDs are positioned on top of a thin QW (dots-on-a-well, D-on-WELL), enabling bias mediated tuning of the response peak wavelength from the MWIR to the LWIR band utilizing two dominating intersubband transitions. The energy level structures of the two detector types were investigated by optical interband measurements and compared to intersubband photocurrent measurements in order to determine the origin of the peaks observed.

The DWELL structures used in this study consist of a 500 nm *n*-doped ($\sim 1 \times 10^{17} \text{ cm}^{-3}$) lower GaAs contact layer, the QD active region and finally the structures are terminated with a 300 nm *n*-doped ($\sim 1 \times 10^{17} \text{ cm}^{-3}$) upper GaAs contact layer. The active region in the dots-in-a-well (D-in-WELL) structure is a ten-layer stack, where each period consists of an undoped InAs QD layer embedded in an 8 nm In_{0.15}Ga_{0.85}As QW and a 33 nm GaAs barrier. The QD layer is inserted asymmetrically in the 8 nm wide QW, with 2 nm In_{0.15}Ga_{0.85}As under and 6 nm In_{0.15}Ga_{0.85}As above the QD layer, respectively. In the D-on-WELL structure, each period in the ten-layer stack consists of a 2 nm In_{0.15}Ga_{0.85}As QW on top of which an undoped InAs QD layer and a 39 nm GaAs barrier are situated, i.e., the upper QW layer was omitted compared to the D-in-WELL. Details about the growth conditions have been described in earlier publications.^{9–11} From atomic force micrographs, a QD density and an average QD diameter and height of $9.3 \times 10^{10} \text{ cm}^{-2}$, 16 and 3.5 nm, respectively, have been revealed. From cross-sectional scanning tunneling microscopy studies of embedded D-in-WELL-structures, it has been observed that the QDs are partially merged with the lower QW layer and that the centers of the QDs are positioned approximately 1.5 nm below the center of the QW.¹¹ Single pixel components (with sizes 170×170 and $360 \times 360 \mu\text{m}^2$) for photocurrent measurements

^{a)}Electronic mail: linda.hoglund@acreo.se.

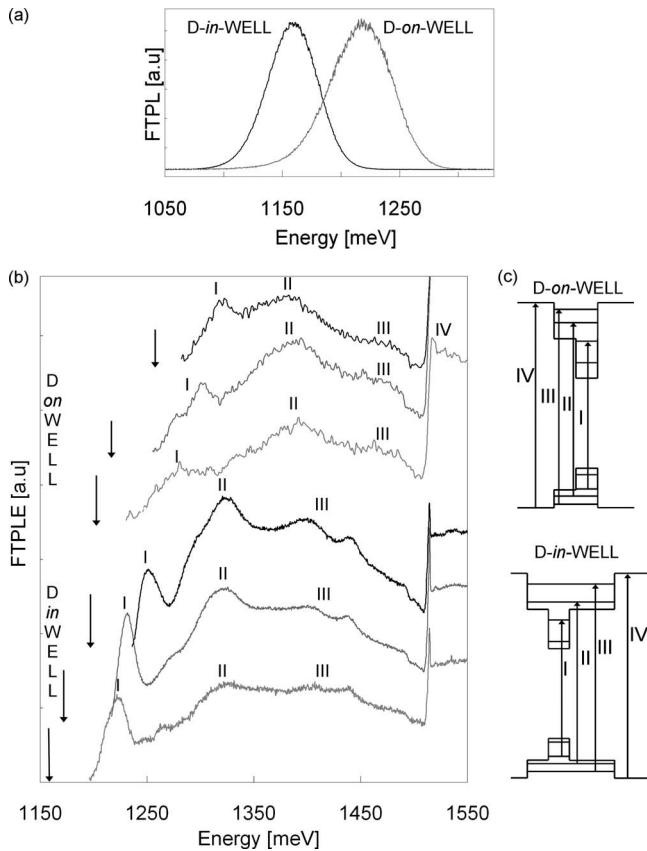


FIG. 1. (a) FTPL spectra (measured at 10 K) of the D-in-WELL and D-on-WELL structure, respectively. The FTPL peak of the D-in-WELL structure is redshifted by 60 meV compared to the D-on-WELL. (b) FTPLE measurements revealing excited energy levels in the QDs (peak I) and in the QW (peaks II and III). The arrows indicate the centers of the detection energy intervals of the six individual FTPLE spectra for the D-on-WELL (the three uppermost spectra) and the D-in-WELL (the three lower spectra). Peak IV corresponds to the GaAs band edge transition. (c) Schematic pictures of the interband transitions corresponding to the peaks I–IV in the FTPLE spectra.

were fabricated by standard optical lithography, etching, and metallization techniques.

The optical characterization of the DWELL structures consisted of two parts: Fourier transform (FT) photoluminescence (FTPL) and related FTPL excitation (FTPLE) spectroscopy¹² and FT photocurrent (FTPC) measurements. The optical measurements of interband transitions were carried out at a temperature of 10 K using a Bomem DA8 FT spectrometer with a liquid nitrogen cooled germanium detector. During the FTPLE measurements, a quartz-halogen tungsten lamp was used as excitation source and the detection window was selected with a SPEX monochromator. For the FTPL measurements, an argon ion laser ($\lambda=514.5$ nm) was used as excitation source. The intersubband photocurrent measurements were also performed in the FT spectrometer, using a globar light source and a Keithley 427 current amplifier. The samples were excited by unpolarized light of normal incidence at a sample temperature of 77 K. All FTPC spectra were normalized with respect to the photon flux to compensate for any variations in the impinging photon flux.

In order to enable interpretations of the origin of the photocurrent, the energy level structure of the DWELLs were unraveled using FTPL and FTPLE measurements (Fig. 1). The average ground state interband transition energy of the D-in-WELL and D-on-WELL structures amounts to 1160

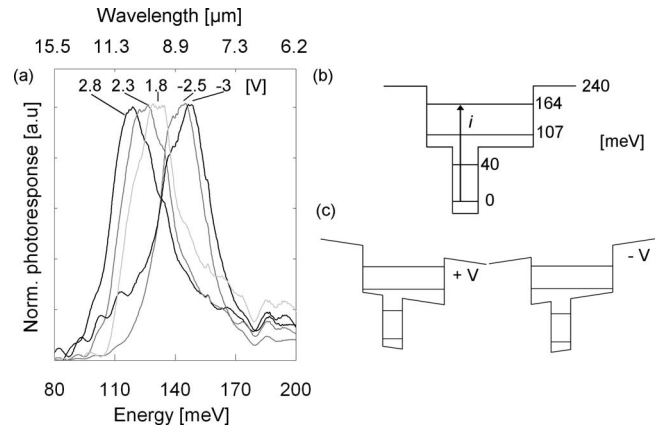


FIG. 2. (a) Photoreponse of the D-in-WELL, which is successively tuned from 120 meV (10.3 μm) to 148 meV (8.4 μm) when changing the magnitude and polarity of the applied bias at a temperature of 77 K. The spectra have been normalized to facilitate comparison of the detection energies. (b) Conduction band energy level scheme derived from the interband measurements (c) The tuning possibility is explained by the asymmetric structure, which allows altering of the separation between the QD and the QW states with different applied biases.

and 1220 meV, respectively, as deduced from FTPL [Fig. 1(a)]. The growth conditions of the QDs in both samples were identical, why the redshift of the FTPL peak in the D-in-WELL should not be due to different size distributions of the QD ensembles in the two structures. More probably, the shift is due to the $\text{In}_{0.15}\text{Ga}_{0.85}\text{As}$ QW layer grown on top of the QD layer. This $\text{In}_{0.15}\text{Ga}_{0.85}\text{As}$ layer acts as a strain reducing layer for the InAs QDs and consequently lowers the energy levels in the QDs.¹³

Excited states in the QDs, as well as in the QWs, were revealed by FTPLE measurements [Fig. 1(b)]. Three detection intervals corresponding to QD ensembles with different ground state energies were chosen for the two structures. The excited states associated with these ground states were deduced from the FTPLE spectra. From the FTPLE measurements of the DWELL structures, it is clear that peak I shifts with the detection energy interval, while peaks II and III remain at the same energy position for each structure. However, when the QW width was changed from 8 nm (D-in-WELL) to 2 nm (D-on-WELL), peaks II and III are blue-shifted by approximately 70 meV. Based on these facts, it can be concluded that peak I is related to QD levels, while peaks II and III are related to QW levels. Peak II is assigned to QW ground state transitions, while peak III is attributed to QW excited state related transitions, in accordance with earlier calculations on QW energy levels.¹⁴ From the different interband measurements, approximate conduction band energy level schemes were deduced in a similar manner as in Ref. 9 [Figs. 2(b) and 3(b)]. The intersubband transitions involved in the photocurrent measurements can then be identified by a comparison of these conduction band energy level schemes with the intersubband photocurrent spectra [Figs. 2(a) and 3(a)].

The photocurrent peak observed for the D-in-WELL is attributed to a transition from the QD ground state to an excited state in the QW, from which the electron tunnels into the matrix [compare Figs. 2(a) and 2(b)]. In a recent study, we have measured the dependence of the tunneling rate on the bias and confirmed that the escape mechanism following a bound-to-bound intersubband transition at low

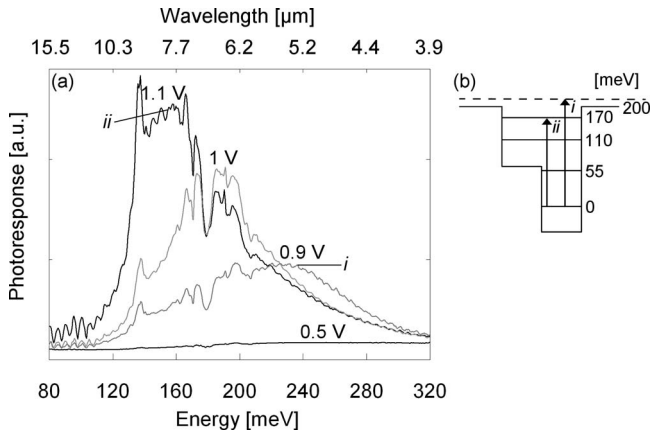


FIG. 3. (a) Photocurrent spectra of the D-on-WELL, which is tuned from 230 meV ($5.4 \mu\text{m}$) to 155 meV ($8 \mu\text{m}$) when changing the applied bias from 0.9 V to 1.1 V at a temperature of 77 K. (b) Conduction band energy level scheme derived from the interband measurements. Two different intersubband transitions (i and ii) are alternatively dominating the photocurrent spectra, as indicated in (b).

temperatures indeed is governed by tunneling through a triangular barrier and that other mechanisms, e.g., thermal emission enhanced by the Poole–Frenkel effect can be neglected.¹⁵ By changing the magnitude and the polarity of the applied bias, we now demonstrate an interesting tuning of the spectral response within the LWIR wavelength window (Fig. 2). By changing the bias applied on the top contact in steps of 0.5 V, from 2.8 to 1.8 V, the peak detection energy is tuned from 120 to 131 meV (10.3 and $9.5 \mu\text{m}$, respectively). When the polarity of the bias is altered to -2.5 and -3 V, the peak energy is shifted to 145 and 148 meV (8.55 and $8.4 \mu\text{m}$), respectively. We attribute this effect to a Stark shift^{16–18} induced in the asymmetrically positioned QD layer embedded in the QW. When a bias is applied, the position of the QD and the QW energy levels will approximately follow the centroid of the QD and the QW, respectively. Due to the asymmetry of the structure, the voltage drop of the two centroids will differ, and consequently a Stark shift will occur. With applied electric fields of the order of ± 65 kV/cm (corresponding to ± 3 V), theoretically predicted Stark shifts of approximately ± 10 meV, compared to the unbiased case, are expected.¹⁶ This is in fairly good agreement with the observed shifts of the photocurrent peak when reversing the applied bias [Fig. 2(a)].

The photocurrent spectra of the D-on-WELL are more complex and seem to involve several intersubband transitions (Fig. 3). At low applied biases (≤ 0.9 V), a proposed intersubband transition from the QD ground state to the GaAs barrier (peak i in Fig. 3) seems to dominate the photocurrent spectra. The magnitude of this peak is almost constant at biases ≥ 0.9 V, which is consistent with the interpretation of final states in the surrounding matrix. At 1 V, a second peak is appearing, most probably emanating from a transition to a QW excited state, and at voltages ≥ 1.1 V this peak [peak ii in Fig. 3(a)] is dominating the photocurrent spectra. The high sensitivity to the applied bias for the second peak is probably due to an increased tunneling probability from the states in the QW with increasing bias.¹⁵ Since the photocurrent spectra for the D-on-WELL are dominated by two different strongly bias-dependent intersubband tran-

sitions, it is actually possible to toggle the detector between the MWIR range (peak at $5.4 \mu\text{m}$) and the LWIR range (peak at $8 \mu\text{m}$). In contrast to the D-in-WELL structure, the spectral response did not change significantly, when the polarity of the bias was reversed. The applied electric field of ± 24 kV/cm (corresponding to ± 1.1 V) would induce a predicted Stark shift of ± 1 – 2 meV, compared to the unbiased case, which is too small to resolve with the widths of the optical bands present.

In conclusion, different ways to tune the detection wavelength have been demonstrated for two different DWELL structures. Tuning within the long wavelength infrared region (between 8.4 and $10.3 \mu\text{m}$) was achieved by reversing the applied bias across an asymmetrical D-in-WELL structure with a QW width of 8 nm. For tuning between the long and medium wavelength infrared regions, two different intersubband transitions were utilized in a D-on-WELL structure. A large shift of the photocurrent peak from 5.4 to $8 \mu\text{m}$ was achieved with a small increase in the applied bias.

The authors would like to thank the Knowledge Foundation and the Swedish Foundation for Strategic Research for support grants and the Swedish Agency for Innovation Systems and the IMAGIC center of excellence for financial support. The authors would also like to thank Stefan Olsson and Stefan Johansson, FLIR Systems and Mattias Hammar, Royal Institute of Technology (KTH) for many fruitful discussions.

¹A. Rogalski, Proc. SPIE **6206**, 62060S (2006).

²A. Köck, E. Gornik, G. Abstreiter, G. Böhm, M. Walthers, and G. Weimann, Appl. Phys. Lett. **60**, 2011 (1992).

³S. D. Gunapala, S. V. Bandara, J. K. Liu, J. M. Mumolo, C. J. Hill, S. B. Rafol, D. Salazar, J. Woolaway, P. D. LeVan, and M. Z. Tidrow, Infrared Phys. Technol. **50**, 217 (2007).

⁴H. C. Liu, J. Li, J. R. Thompson, Z. R. Wasilewski, M. Buchanan, and J. G. Simmons, IEEE Electron Device Lett. **14**, 566 (1993).

⁵K.-K. Choi, C. Monroy, V. Swaminathan, T. Tamir, M. Leung, J. Devitt, D. Forrai, and D. Endres, Infrared Phys. Technol. **50**, 124 (2007).

⁶M. Kaldirim, S. U. Eker, Y. Arslan, U. Tumkaya, and C. Besikci, IEEE Photonics Technol. Lett. **20**, 709 (2008).

⁷S. Krishna, S. Raghavan, G. von Winckel, P. Rotella, A. Stintz, C. P. Morath, D. Le, S. W. Kennerly, Appl. Phys. Lett. **82**, 2574 (2003).

⁸E. Varley, M. Lenz, S. J. Lee, J. S. Brown, D. A. Ramirez, A. Stintz, S. Krishna, A. Reisinger, and M. Sundaram, Appl. Phys. Lett. **91**, 081120 (2007).

⁹L. Höglund, P. O. Holtz, C. Asplund, Q. Wang, S. Almqvist, H. Malm, E. Petrini, H. Pettersson, and J. Y. Andersson, Appl. Phys. Lett. **88**, 213510 (2006).

¹⁰L. Höglund, E. Petrini, C. Asplund, H. Malm, J. Y. Andersson, and P. O. Holtz, Appl. Surf. Sci. **252**, 5525 (2006).

¹¹L. Ouattara, A. Mikkelsen, E. Lundgren, L. Höglund, C. Asplund, and J. Y. Andersson, J. Appl. Phys. **100**, 044320 (2006).

¹²J. Dalfors, T. Lundström, P. O. Holtz, H. H. Radamson, B. Monemar, J. Wallin, and G. Landgren, J. Appl. Phys. **80**, 6855 (1996).

¹³T. Kakitsuka, T. Saito, T. Nakaoka, Y. Arakawa, H. Ebe, M. Sugawara, and Y. Yoshikuni, Phys. Status Solidi C **0**, 1157 (2003).

¹⁴G. Arnaud, J. Allègre, P. Lefebvre, H. Mathieu, L. K. Howard, and D. J. Dunstan, Phys. Rev. B **46**, 15290 (1992).

¹⁵L. Höglund, P. O. Holtz, H. Pettersson, C. Asplund, Q. Wang, S. Almqvist, S. Smuk, E. Petrini, and J. Y. Andersson, Appl. Phys. Lett. **93**, 103501 (2008).

¹⁶P. F. Yuh and K. L. Wang, IEEE J. Quantum Electron. **25**, 1671 (1989).

¹⁷Y. J. Mii, R. P. G. Karunasiri, K. L. Wang, M. Chen, and P. F. Yuh, Appl. Phys. Lett. **56**, 1986 (1990).

¹⁸P. Aivaliotis, N. Vukmirovic, E. A. Zibik, J. W. Cockburn, D. Indjin, P. Harrison, C. Groves, J. P. R. David, M. Hopkinson, and L. R. Wilson, J. Phys. D **40**, 5537 (2007).